OBC
www.rsc.org/obc

Time-dependent complex formation of dendritic poly(L-lysine) with plasmid DNA and correlation with *in vitro* transfection efficiencies

Tatsuya Okuda,[a] Satoru Kidoaki,[b] Mio Ohsaki,[a] Yoshiyuki Koyama,[c] Kenichi Yoshikawa,[b] Takuro Niidome*[a] and Haruhiko Aoyagi[a]

[a] *Department of Applied Chemistry, Faculty of Engineering, Nagasaki University, Nagasaki 852-8521, Japan*

[b] *Department of Physics, Graduate School of Science, Kyoto University, Core Research for Evolutional Science and Technology (CREST) of Japan Science and Technology Corporation, Kyoto 606-8502, Japan*

[c] *Department of Home Economics, Otsuma Women's University, Chiyoda-ku, Tokyo, 102-8357, Japan*

Received 6th December 2002, Accepted 10th March 2003
First published as an Advance Article on the web 25th March 2003

Dendritic poly(L-lysine) of the 6th generation shows high transfection efficiency into several cultivated cells with low cytotoxicity. In order to understand the mechanism of complex formation with plasmid DNA, the complex was observed using atomic force microscopy. After mixing for 15 min, 1–2 μm assemblies of complexes composed of several small particles (50–200 nm) were observed. At the same time, individual small complexes of 50 to 500 nm were observed on a mica surface. After incubation for 2 h, only the large complexes were found on the mica surface. As a result of further dynamic light scattering analysis and measurement of the transfection efficiency at different time points, the transfection efficiency of KG6 was found to increase with increasing size of the DNA-complexes. This result indicates that large complexes of more than 1 μm are major species that contribute to transfection *in vitro*.

Introduction

The development of efficient non-viral gene delivery techniques is one of the important themes for gene therapy.[1] On the other hand, these techniques are also powerful tools to reveal gene functions in cells and organs in the fields of genomics and proteomics. During various efforts to improve the transfection efficiency and understand the mechanism for major gene carriers, such as cationic lipids and polymers, several kinds of dendritic molecules were recently reported as novel gene carriers. First of all, the use of the polyamideamine (PAMAM) dendrimer was reported.[2,3] Subsequently, in order to improve the transfection efficiency, several derivatives of PAMAM dendrimer, *e.g.*, partially degraded-PAMAM dendrimer,[4] PAMAM dendrimer modified by cyclodextrins,[5] and PAMAM dendrimer synthesized from a cyclic core,[6] were reported. On the other hand, other types of dendrimers were reported as gene carrier molecules. A dendrimer consisting of L-lysines as a branch unit was introduced by Choi *et al.*[7,8] They synthesized several types of block copolymers consisting of poly(ethylene glycol) and poly(L-lysine) dendrimers, and reported the DNA-binding manner of the molecules. Shah *et al.* also reported that amphipathic asymmetric poly(L-lysine) dendrimers, in which the dendritic structure was attached to an amino group of α-amino myristic acid, had the ability to transfer genes into cells without significant cytotoxicity.[9] Furthermore, polypropylenimine dendrimers and a dendrimer containing phosphorus as a branch core were reported by Zinselmeyer *et al.*[10] and Loup *et al.*,[11] respectively.

Recently, we reported that mono-dispersed dendritic poly(L-lysine) made of hexamethylenediamine as an initiator core showed high transfection efficiency into several cultivated cells with low cytotoxicity (Fig. 1).[12] Interestingly, the DNA-complex of this dendrimer had a low zeta-potential (+3 mV), and showed high transfection efficiency even in the presence of 50% serum. From these characters, this molecule has been expected to be a candidate for a gene carrier molecule that works *in vivo* with high efficiency. With regard to the mechanism of gene transfection into cells *in vitro*, it has been suggested that the dendrimer forms a complex with plasmid DNA, and the complex is incorporated *via* the endocytosis pathway. After that, a part of the complex would escape from the endocytotic vesicle by the proton sponge effect of the dendrimer, like a polyethylenimine,[13] and then, the gene encoded in the plasmid DNA would be expressed after transport into the nucleus. Although various efforts have been made to understand the mechanism, the details have not yet been fully understood, as is the situation for other general carrier molecules such as cationic lipids and polymers.

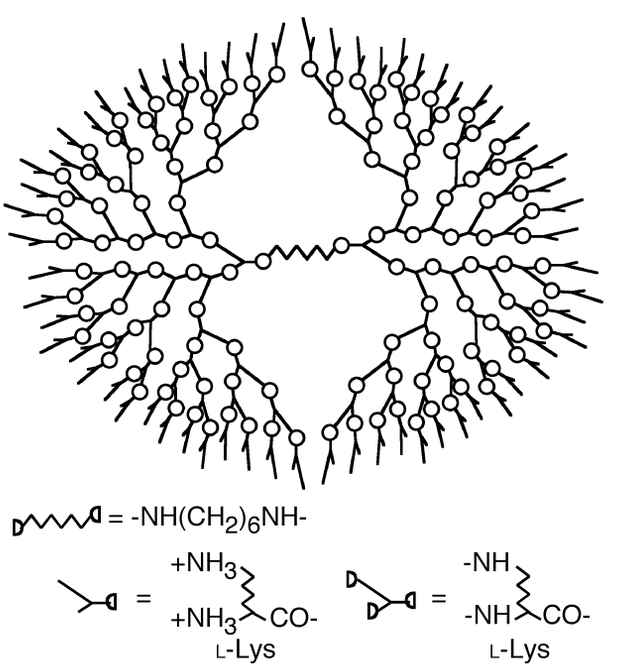

Fig. 1 Structure of dendritic poly(L-lysine) of the 6th generation (KG6).

In this study, we focused on the structure of the DNA-complex of the dendritic poly(L-lysine) of the 6th generation (abbreviated to KG6, Fig. 1) and its relationship to transfection efficiency. The detailed structure and size of the complex were

DOI: 10.1039/b212086k

observed by atomic force microscopy and dynamic light scattering, and the transfection efficiency was evaluated by luciferase expression. Subsequently, we could find a clear correlation between the size of complex and the transfection efficiency *in vitro*.

Results and discussion

Structure of the DNA-complex of KG6

To clarify the detailed structure of the DNA complex of KG6, we employed a fluorescence-microscope-coupled atomic force microscope (FM–AFM). This system enabled us to observe the fluorescent image of the complex and the AFM image at the same time and position. After incubation of the plasmid DNA and KG6 in DMEM (pH 7.2) for 15 min, 1–2 μm assemblies of complexes were observed in the fluorescence image (Fig. 2A). In the AFM image, these complexes could be observed in similar sizes and shapes (Fig. 2B). From the magnified image of a complex surface, this large complex consisted of several small particles (50–200 nm) (Fig. 2C). On the other hand, we found a lot of small particles which were uniformly adsorbed all over the mica surface only through the AFM observation (Fig. 2D), since FM could not visualize the individual small particles due to their small size and markedly weak fluorescence. As a result of magnifying the surface, spherical and extended complexes were observed, and their sizes were 50 nm in diameter, and 50 and 500 nm in width and length, respectively. It is likely that these small particles are condensates consisting of single, or a few, molecules of the plasmid DNA. After incubation for 2 h, complexes of several μm were observed (Fig. 2E). These large complexes also consisted of small particles (Fig. 2F). However, no small particles, which were observed in the case of the 15 min incubation, could be found on the mica surface (Fig. 2E and F). This result suggests that after mixing the plasmid DNA and KG6, KG6 first binds to the plasmid DNA and makes the DNA condense into small particles composed of single, or a few, DNA molecules. Second, the small particles associate together, and then grow into large aggregates of several μm.

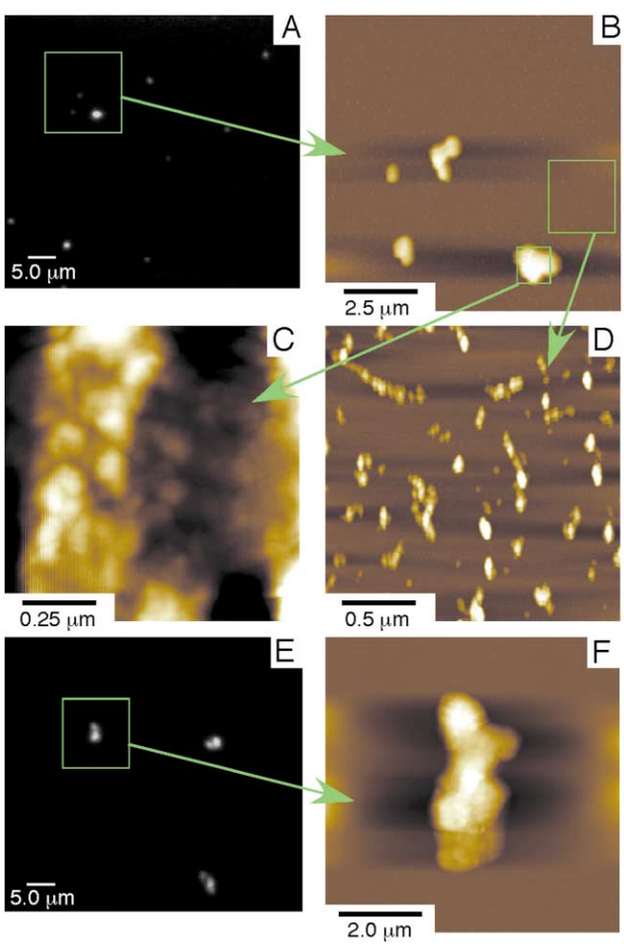

Fig. 2 Fluorescence and AFM images of DNA-complexes of KG6. Panels A and E are fluorescence images of the complexes after 15 min and 2 h incubation, respectively. Panel B is the AFM image of the area indicated by a green square in Panel A. Panel C is a magnified image of the surface of the large complex (>1 μm) indicated by a green square in Panel B. Panel D is a magnified image of the small complexes (<1 μm) on the mica surface indicated by a green square in Panel B. Panel F is the AFM image of the area indicated by a green square in Panel E.

Size distribution of the DNA complexes of KG6

To evaluate the time-dependent growth of the complexes, we measured the size distribution of the complexes at different time points using dynamic light scattering of the particle size. After mixing the plasmid DNA and KG6 in DMEM for 5 min, particles of about 500 nm were mainly detected (Fig. 3). After the 15 min incubation, the size was slightly increased. The size of the initial complex corresponded to the result of the AFM (Fig. 2D). In the results of the AFM, large complexes (>1 μm) were observed (Fig. 2B). However, in the dynamic light scattering analysis, we did not observe such large complexes. The reason is that the large complexes stood out under fluorescence microscopy (Fig. 2A), and as a result, we focused on these large complexes in the AFM. In fact, their population would be negligible compared with that of the small complexes (<1 μm) at this time point (15 min). After that, the diameters of the complexes became larger. The inset in Fig. 3 shows that the mean diameter of the complexes increased in a time-dependent manner. After 2 h incubation, 70% of the complexes had a large diameter of more than 1 μm. This size of complex corresponded to that of the large complexes observed in the AFM after incubation for 2 h (Fig. 2F).

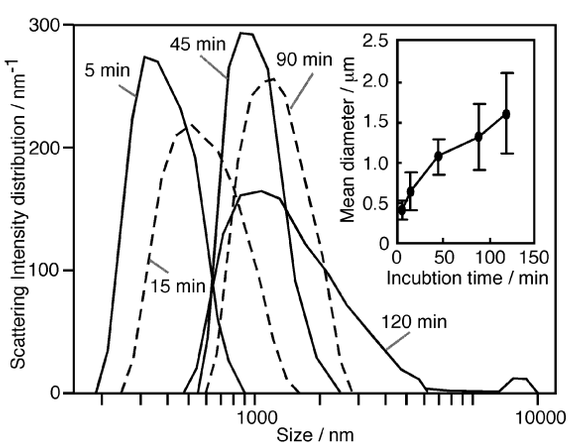

Fig. 3 Dynamic light scattering analysis of DNA-complexes of KG6. KG6 was incubated with the plasmid DNA in DMEM for 5 min to 2 h at room temperature, and then dynamic light scattering was measured at 25 °C. The inset shows the time-dependent change in the mean diameter of the complexes.

Next, we discuss the growth profile in Fig. 3. In our sample, particles fuse with larger particles through collision at a certain probability. The probability will be dependent on the manner of interaction: repulsion on a long range due to the charge effect and attraction on a small range due to the contact interaction. Thus, the growth rate of the particles is given as the multiplication of the density of particles ($N(t)/V$), the mass of the particle (m) and the surface area ($m^{2/3}$) according to the following formula (m: mass of a particle; $N(t)$: number of particles; V: solution volume):

$$\frac{dm}{dt} \propto \frac{N(t)}{V} m \bullet m^{2/3} \qquad (1)$$

Since the product of the number and mass of the particle is constant ($N(t) \times m = M$),

$$\frac{dm}{dt} \propto \frac{M}{V} m^{2/3} \quad (2)$$

After integration by taking $k = M/V$,

$$m^{1/3} \approx kt + c \quad (3)$$

$$D \approx kt + c \quad (4)$$

Eqn. (4) is given by assuming the relationship, $m \propto D^3$ where D is the diameter of the particle. From this calculation, the growth of the particle should be proportional to time. Actually, we observed a linear correlation between time and diameter at times of less than 50 min (Fig. 3, inset). After that, the growth rate decreased. This difference would be due to the adsorption/precipitation of the large complexes on the cuvette surface, which could not be detected by the light scattering analysis.

Time-dependent transfection efficiency

Which size of complex has an advantage for uptake into cells and gene expression? To answer this question, the transfection efficiency at different time points of incubation was measured. KG6 was pre-incubated with the plasmid DNA in DMEM for 0 to 2 h at room temperature in a test tube, and then the mixture was added to cultured cells. After incubation for 15 min to 6 h at 37 °C, the mixture was replaced with fresh DMEM containing 10% FBS, and the cells were further incubated for 24 h. The cells were harvested and the transfection efficiency was estimated by measuring the luciferase activity. As shown in Fig. 4A, the transfection efficiency was increased by increasing the pre-incubation time in the case of a short incubation with cells [○ (15 min), ◇ (30 min) and □ (1 h)]. In the case of incubation for more than 2 h (●, ◆ and ■), high transfection efficiencies were observed even in the case of a short pre-incubation time. Since the complexes grow over a few hours as described above, this result suggests that bigger complexes would be advantageous for transfection. On the other hand, the transfection efficiencies were independent of the pre-incubation time. A longer incubation with the cells allowed the complexes to grow into larger aggregates in the medium, and then they would be incorporated into the cells. If so, the transfection efficiency should correlate with the total incubation time (pre-incubation time in tube + incubation time with cells). As a result of a re-plot of these data against the total incubation time and the transfection efficiency, both of them correlated well (Fig. 4B). As no small complexes (<500 nm) were observed after 2 h incubation in the AFM images, the slow increase in the transfection efficiency after 2 h would reflect the trafficking efficiency downstream from the uptake of the complexes to gene expression. The rapid increase until 2 h of incubation would reflect the maturation of the complexes to larger sizes (>1 μm).

In this study, we could find a clear correlation between complex size and gene expression. Our data suggest that large complexes of more than 1 μm had an advantage for gene expression. A similar result has been already reported by Emi *et al.*[14] They used poly-L-arginine (M_r = 139,200) and made different sizes of DNA-complexes by mixing at different charge ratios. As a result of measuring the transfection efficiency of each complex, large complexes (>5 μm) showed higher transfection efficiency than smaller complexes (<1 μm). Ross and Hui also reported that cell association and uptake into cells, and transfection efficiency of lipoplex were increased with increasing lipoplex size.[15] In their case, they controlled the size of the complexes by adding polyanions, and obtained a clear correlation between the size and the activities with cells. In our case, we tried to plot a time-course of the complex size and transfection efficiency

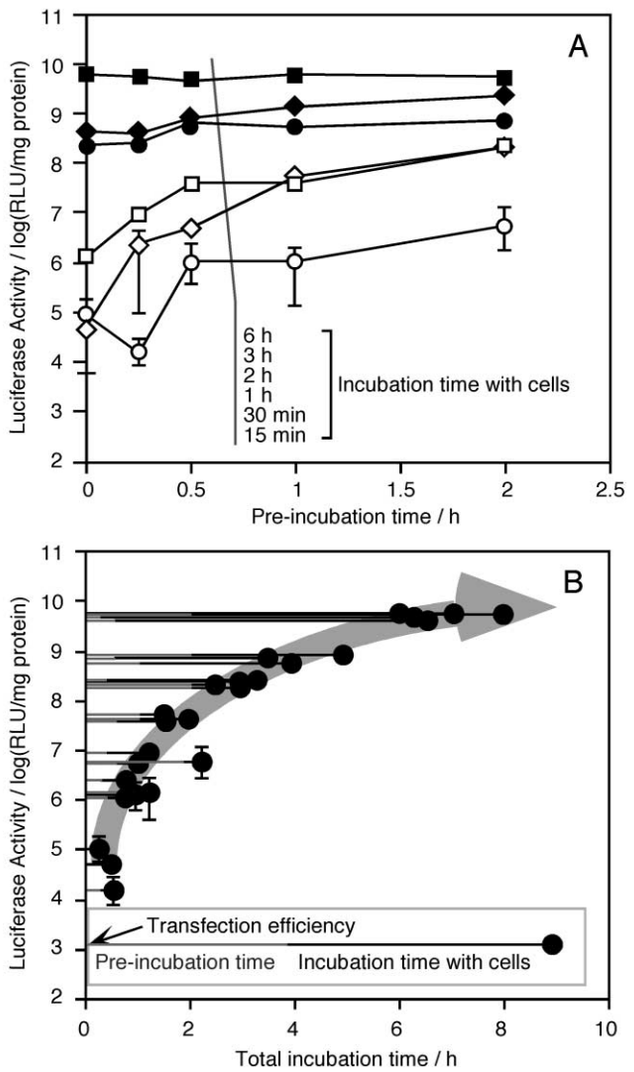

Fig. 4 Time-dependent transfection efficiency of KG6. KG6 was pre-incubated with the plasmid DNA in DMEM for 0 to 2 h at room temperature, and then the mixture was added to cultured cells (CHO cells). After incubation for 15 min to 6 h at 37 °C, the mixture was replaced with fresh DMEM containing 10% FBS, and the cells were further incubated for 24 h. The cells were harvested and the transfection efficiency was estimated by measuring the luciferase activity. Panel A shows the relationship between the pre-incubation time and the transfection efficiency. The efficiencies as the result of incubation with the cells for 6, 3, 2, 1, 0.5, and 0.25 h are indicated by ■, ◆, ●, □, ◇, and ○, respectively. Panel B shows the relationship between the total incubation time and the transfection efficiency. Gray and black lines indicate the pre-incubation and incubation times with cells, respectively. The height of the ● indicates the transfection efficiency of each incubation condition.

because we wanted to compare them in the same composition and condition. The only variable factor was time, and not the concentration of the samples and other additives, which may cause an unexpected influence on the transfection process. Fortunately, as the growth of the complexes to the optimum size for transfection was a slow process, we identified a time-dependent increase in the transfection efficiency and got a clear correlation between them.

Furthermore, we found an interesting growth mechanism of the complexes using AFM. After mixing the DNA and KG6, small complexes were immediately formed within several minutes, and then further aggregation occurred, keeping the spherical shape of the small complex unit. In the case of lipoplex, reconstitution of the lipid occurred after mixing of the liposome and DNA since assembly of liposomes is promoted by many cationic lipids as a result of hydrophobic interactions.[16]

However, since KG6 is a polycation, the dynamic reconstitution of the initial complexes observed in the case of lipoplex would not be found. This difference in the mode of complex formation would cause a different transfection manner of cationic liposome- and polycation-mediated transfections.[17] In this report, we detailed the formation of complexes of a cationic dendrimer and plasmid DNA. These results will provide important information for the development of functional gene carriers for gene therapy and gene transfection in molecular biology.

Experimental

Chemicals

Plasmid DNA (pCMV-Luc) was constructed by subcloning the HindIII/XbaI firefly luciferase cDNA fragment from the pGL3-control vector (Promega, Madison, WI, USA) into the polylinker of the pcDNA3 vector (Invitrogen, Carlsbad, CA, USA). pDNA was amplified in the *Escherichia coli* strain DH5α, isolated, and purified using a QIAGEN Plasmid Giga Kit (QIAGEN GmbH, Hilden, Germany). DMEM (Dulbecco's modified Eagle's medium, pH 7.2) and FBS (fetal bovine serum) were purchased from IWAKI GLASS (Chiba, Japan).

Fluorescence and atomic force microscopy

The structure of complexes between plasmid DNA and KG6 was observed with a fluorescence-microscope-coupled atomic force microscope (NVB100, Olympus, Japan), according to the following procedure: (1) 40 μL of KG6 solution (3.2 mM of amine in HBS) was diluted to 940 μL of DMEM, and then 20 μL of DNA solution (1.6 mM of phosphates in HBS) was mixed slowly at room temperature. Final concentrations of KG6 and plasmid DNA were 128 μM of the amines and 32 μM of the phosphates, respectively. After incubation for 15 min or 2 h, the fluorescent dye 4′,6-diamidino-2-phenylindole (DAPI 32 μM), and 2-mercaptoethanol (4% (v/v)) as an antioxidant, were added to the solution to visualize the complex structure in the medium. The descriptions of the concentrations are the final concentrations. (2) Newly cleaved thin mica (thickness: *ca.* 30–50 μm) was closely stuck to a cover glass plate (Matsunami Glass, No.1, Japan) for FM observation with an oil-immersed 100× objective lens (short working distance). (3) The fluorescently-stained complexes were observed in a sample droplet (10 μl) instilled on the mica glued on cover glass with the aid of an ultra-weak-light detectable CCD camera (EB-CCD, Hamamatsu Photonics, Japan). (4) The adsorption process of the complexes from the bulk medium to the mica surface was monitored to ensure the presence of adsorbed complexes for AFM observation. (5) The sample droplet on the mica was removed by nitrogen-blowing, and the mica was washed with Millipore water, and dried again by nitrogen-blowing. (6) Finally, the complexes selected by FM observation were observed with the tapping mode of the AFM. Both FM and AFM images could be obtained on the same complex.

Particle size analysis

Samples were prepared by mixing plasmid DNA and KG6 as described above. After 5 min to 2 h, dynamic light scattering was analyzed using an Electrophoretic Light Scattering Spectrophotometer ELS-8000 (Otsuka Electronics Co. Ltd.). The mean diameter and size distribution were computed using functions supplied with the instrument. In order to avoid non-specific adsorption of complexes to the quartz cuvette, the cuvette (1 × 1 cm) was siliconized.

Cell culture and transfection

A Chinese hamster ovary cell line (CHO, RCB accession no. RCB0285) was purchased from RIKEN Cell Bank (Tsukuba, Japan). The cells were cultivated in DMEM supplemented with 10% FBS and antibiotics (30 μg mL^{-1} kanamycin sulfate) at 37 °C in a humidified atmosphere containing 5% CO_2. The cells were plated at a density of 1.0×10^5 cells $well^{-1}$ 48 h prior to transfection in a 24-well plate.

Just before the transfection procedure, the cells in the 24-well plate were washed with 1 mL of serum-free medium. Complexes were prepared by mixing plasmid DNA and KG6 as described above. After standing for 0–2 h at room temperature, the KG6–DNA mixture was poured gently onto the cells. After incubation for 15 min–6 h at 37 °C, the medium was replaced with 1 ml of fresh DMEM containing 10% FBS, and the cells were further incubated for 24 h. The harvesting of the cells and the luciferase assays were performed as described in the protocol of the PicaGene luminescence kit (TOYO B-Net Co. Ltd, Tokyo, Japan). Luciferase relative light units (RLU) were analyzed by a luminometer (Maltibiolumat LB9505, Berthold, Germany). The protein concentrations of the cell lysates were measured by the Bradford assay using bovine serum albumin as the standard.[18] The light unit values shown in the figures represent the specific luciferase activity (RLU mg^{-1} protein), which was standardized for the total protein content of the cell lysate. The measurement of gene transfer efficiency was performed in triplicate.

Acknowledgments

This research was supported by Grants-in-aid from the Ministry of Education, Culture, Sports, Science and Technology of Japan (no. 12217115 and no. 14703033), from the Foundation Advanced Technology Institute, and from the Nagasaki Advanced Technology Development Council. We acknowledge the technical support of Dr Takeo Hyodo of the Department of Materials Science and Engineering, Faculty of Engineering, Nagasaki University, Nagasaki, Japan, in performing the particle size analysis.

References

1 M. Nishikawa and L. Huang, *Hum. Gene Ther.*, 2001, **12**, 861–870.
2 J. Haensler and F. C. Szoka, *Bioconjugate Chem.*, 1993, **4**, 372–379.
3 J. F. Kukowska-Latallo, A. U. Bielinska, J. Johnson, R. Spindler, D. A. Tomalia and J. R. Jr. Baker, *Proc. Natl. Acad. Sci. USA*, 1996, **93**, 4897–4902.
4 J. Haensler and F. C. Szoka, *Bioconjugate Chem.*, 1993, **4**, 372–379.
5 H. Arima, F. Kihara, F. Hirayama and K. Uekama, *Bioconjugate Chem.*, 2001, **12**, 476–84.
6 H. Cheng, R. Zhou, L. Liu, B. Du and R. Zhou, *Genetica*, 2000, **108**, 53–56.
7 J. S. Choi, E. J. Lee, Y. H. Choi and J. S. Park, *Bioconjugate Chem.*, 1999, **10**, 62–65.
8 J. S. Choi, D. Joo, C. H. Kim, K. Kim and J. S. Park, *J. Am. Chem. Soc.*, 2000, **122**, 474–480.
9 D. S. Shah, T. Sakthivel, I. Toth, A. T. Florence and A. F. Wilderspin, *Int. J. Pharm.*, 2000, **208**, 41–48.
10 B. H. Zinselmeyer, S. P. Mackay, A. G. Schatzlein and I. F. Uchegbu, *Pharm. Res.*, 2002, **19**, 960–967.
11 C. Loup, M.-A. Zanta, A.-M. Caminade, J.-P. Majoral and B. Meunier, *Chem. Eur. J.*, 1999, **5**, 3644–3650.
12 M. Ohsaki, T. Okuda, A. Wada, T. Hirayama, T. Niidome and H. Aoyagi, *Bioconjugate Chem.*, 2002, **13**, 510–517.
13 O. Bousiff, F. Lezoualc'h, M. A. Zanta, M. D. Mergny, D. Scherman, B. Demeneix and J.-P. Behr, *Proc. Natl. Acad. Sci. USA*, 1995, **92**, 7279–7301.
14 N. Emi, S. Kidoaki, K. Yoshikawa and H. Saito, *Biochem. Biophys. Res. Commun.*, 1997, **231**, 421–424.
15 P. C. Ross and S. W. Hui, *Gene Ther.*, 1999, **6**, 651–659.
16 P. Harvie, F. M. P. Wong and M. B. Bally, *Biophys. J.*, 1998, **75**, 1040–1051.
17 K. Yoshikawa and Y. Yoshikawa, Compaction and condensation of DNA, in *Pharmaceutical Perspectives of Nucleic Acid-Based Therapeutics*, ed. R. I. Mahato and S. W. Kim, Taylor & Francis, 2002, 137–163.
18 M. M. Bradford, *Anal. Biochem.*, 1976, **72**, 248–254.